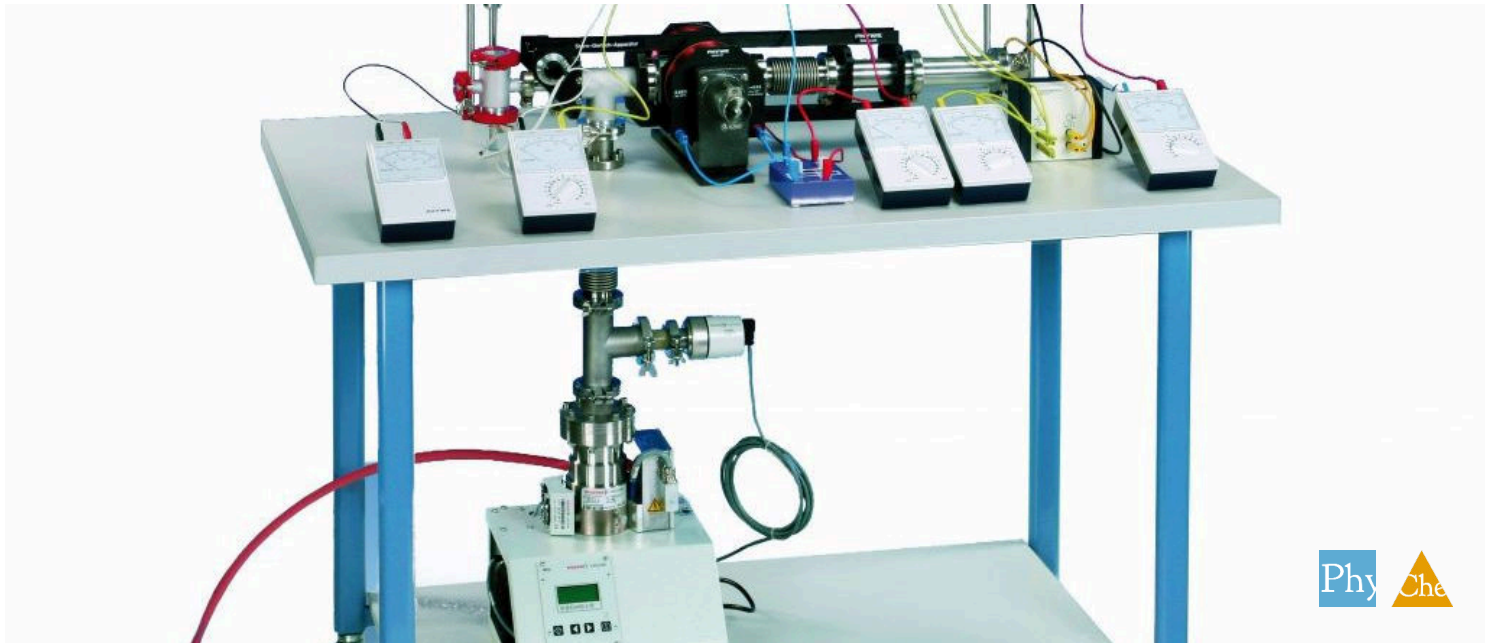


Stern-Gerlach experiment



The goal of this experiment is to investigate the quantisation of the angular momentum.

Physics

Modern Physics

Quantum physics

Physics

Modern Physics

Atomic & Molecular Physics

Chemistry

Physical chemistry

Atomic structures & properties



Difficulty level

easy



Group size

1



Preparation time

10 minutes



Execution time

10 minutes

PHYWE
excellence in science

General information

Application

PHYWE
excellence in science

Setup

The Stern–Gerlach experiment demonstrated that the spatial orientation of angular momentum is quantized. Thus an atomic-scale system was shown to have intrinsically quantum properties. In the original experiment, silver atoms were sent through a spatially varying magnetic field, which deflected them before they struck a detector screen, such as a glass slide. Particles with non-zero magnetic moment are deflected, due to the magnetic field gradient, from a straight path. The screen reveals discrete points of accumulation, rather than a continuous distribution, owing to their quantized spin. Historically, this experiment was decisive in convincing physicists of the reality of angular-momentum quantization in all atomic-scale systems.

Other information (1/2)

PHYWE
excellence in science

Prior knowledge



The prior knowledge required can be found in the theory section.

Scientific principle



A beam of potassium atoms generated in a hot furnace travels along a specific path in a magnetic two-wire field. Because of the magnetic moment of the potassium atoms, the non-homogeneity of the field applies a force at right angles to the direction of their motion. The potassium atoms are thereby deflected from their path.

By measuring the density of the beam of particles in a plane of detection lying behind the magnetic field, it is possible to draw conclusions as to the magnitude and direction of the magnetic moment of the potassium atoms.

Other information (2/2)

PHYWE
excellence in science

Learning objective



The goal of this experiment is to investigate the quantisation of the angular momentum.

Tasks



1. Recording the distribution of the particle beam density in the detection plane in the absence of the effective magnetic field.
2. Fitting a curve consisting of a straight line, a parabola, and another straight line, to the experimentally determined special distribution of the particle beam density.
3. Determining the dependence of the particle beam density in the detection plane with different values of the non-homogeneity of the effective magnetic field.
4. Investigating the positions of the maxima of the particle beam density as a function of the non-homogeneity of the magnetic field.

Theory (1/31)

Magnetic moment

Investigating the positions of the maxima of the particle beam density as a function of the non-homogeneity of the magnetic field.

$$\vec{\mu} = -\frac{e}{2m_0} g_s \cdot \vec{S}$$

If one considers the component S_z of the spin in a given z-direction, the system has two different possible orientations, characterized by the quantum numbers

$$m_s = \pm \frac{1}{2}$$

The z-component of spin takes the eigen value

$$S_z = m_s \hbar$$

Theory (2/31)

The associated magnetic moment in the z-direction take the value

$$\mu_z = -\frac{e\hbar}{2m_0} = -\mu_B \cdot m$$

with the Bohr magneton

$$\mu_b = -\frac{e\hbar}{2m_0} = -9.248 \cdot 10^{-24} \text{ Am}^2$$

and $m = m_s \cdot g_s$

The literature value of the g-factor is

$$g_s = 2.0024 \cdot (2)$$

Theory (3/31)

Hence, $m = \pm 1.0012 \approx \pm 1$ (3)

The object of the Stern-Gerlach experiment is to establish the directional quantization of the electron spin. Furthermore, according to which quantity is taken as known, the value of μ_z ; μ_B ; m or g_s can be determined.

Let the direction of the magnetic field with field strength \vec{H} and induction \vec{B} entered by the potassium atoms be taken as z-coordinate. The outer electrons of the potassium atom complete a classical precessional movement about the field direction. The eigen values of the magnetic moment are therefore parallel or antiparallel to the magnetic field:

$$\vec{\mu}_H = \mu_z \frac{\vec{H}}{H} = -m \cdot \mu_B \frac{\vec{H}}{H} \quad (4)$$

Theory (4/31)

Action of forces

The forces acting on the potassium atom are attributable to their magnetic moment and arise when the field is inhomogeneous:

$$\vec{F} = (\mu_H \overset{\rightarrow}{grad}) \vec{B} = \mu_0 (\vec{\mu}_H \overset{\rightarrow}{grad}) \vec{H}$$

The expression in parentheses is to be understood as a scalar product whose differential operators act on \vec{B} or \vec{H} . The force is therefore determined by the vector gradient of the magnetic field:

$$\vec{F} = \mu_0 \mu_H \left(\frac{\vec{H}}{H} \overset{\rightarrow}{grad} \right) \vec{H}$$

Theory (5/31)

To simplify this equation, we fall back upon the identity

$$\frac{1}{2} \text{grad } H^2 = \left(\vec{H} \text{ grad} \right) \vec{H} + \vec{H} \times \vec{\text{curl}} H$$

in which the vector product of \vec{H} and $\vec{\text{curl}} H$ vanishes since

$$\vec{\text{curl}} H = 0$$

Further, we can put

$$\frac{1}{2} \text{grad } \vec{H}^2 = \frac{1}{2} \text{grad } H^2 = \vec{H} \text{ grad } H$$

Theory (6/31)

i.e., only the numerical values H of the magnetic field as a scalar are decisive:

$$\vec{F} = \mu_0 \mu_H \text{grad} H = \mu_H \text{grad} B$$

For example, when using a cartesian system of coordinates (x, y, z) , the component of the force acting on the potassium atom in the z -direction equals

$$F_z = \mu_H \frac{\partial B}{\partial z} \text{ or } F_z = -m \mu_H \frac{\partial B}{\partial z} \quad (5)$$

Assuming that the potassium atoms enter the magnetic field at right angles to it and leave it again after a path Δl , and that $\partial B / \partial z$ is constant, the potassium atoms describe a parabolic path and are deflected more or less strongly in the z -direction according to their different velocities of entry, with corresponding changes in direction. The position of the plane $z = 0$ in the magnetic field must still be determined accurately.

Theory (7/31)

To produce an inhomogeneous magnetic field, one starts with the shape of pole piece shown in Fig. 1.

So long as the magnetization does not proceed to saturation, the pole pieces, of circular cylindrical form, lie in two equipotential surfaces of a two-wire system using currents in opposite directions. The magnetic field \vec{H} therefore consists of two components, \vec{H}_1 and \vec{H}_2 as shown in Fig. 2:

$$\vec{H}(\vec{r}) = \vec{H}_1(\vec{r}) + \vec{H}_2(\vec{r})$$

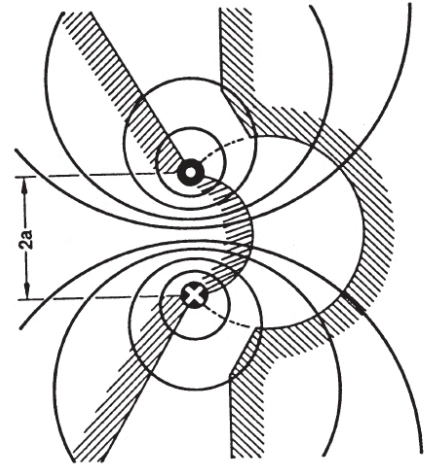


Fig. 1: Two-wire field.

Theory (8/31)

Each of the two conductors contributes to the field as follows:

$$\vec{H}_i(\vec{r}_i) = \frac{\vec{l}_i \times \vec{r}_i}{2\pi r_i^2}, (i = 1, 2)$$

where $\vec{l}_1 = -\vec{l}_2 = \vec{l}$

is the excitation current for the magnetic fields. Hence, at the point \vec{r} ,

$$\vec{H}(\vec{r}) = \frac{2}{2\pi} \vec{l} \times \left(\frac{\vec{r}_1}{r_1^2} - \frac{\vec{r}_2}{r_2^2} \right)$$

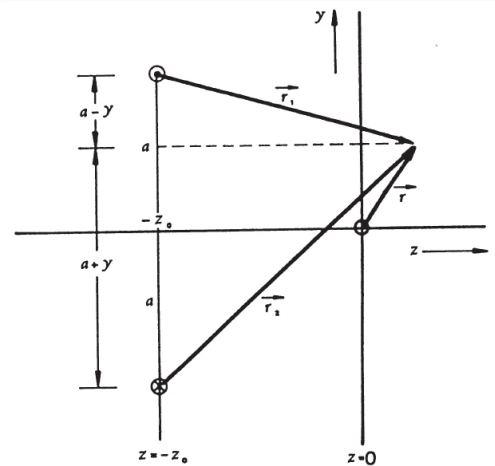


Fig. 2: Determination of a system of coordinates.

Theory (9/31)

The value of the magnetic field strength is obtained by squaring this expression. Remembering in the subsequent calculation that \vec{r}_1 and \vec{r}_2 lie in a plane at right angles to l , one finally obtains:

$$H = \frac{l}{\pi} \frac{a}{r_1 r_2} \quad (6)$$

The change in the value of H as a function of z can be calculated, using

$$r_1^2 = (a - y)^2 + (z + z_0)^2$$

$$\text{and } r_2^2 = (a + y)^2 + (z + z_0)^2$$

$$\text{as } \frac{\partial H}{\partial z} = -\frac{l \cdot a(z+z_0)^2}{\pi} \cdot \frac{(r_1^2 + r_2^2)}{r_1^3 r_2^3} = -\frac{2l \cdot a(z+z_0)^2}{\pi} \cdot \frac{a^2 + y^2 + (z+z_0)^2}{((a^2 - y^2)^2 + 2(z+z_0)^2 \cdot (a^2 + y^2) + (z+z_0)^4)^{3/2}} \quad (7)$$

Theory (10/31)

The surfaces of constant field inhomogeneity are shown in Fig. 3.

The equipotential surfaces in the neighbourhood of $z = z_1$, are to be regarded as planes, to a good approximation.

We must now find the plane $z = z_1$, in which the equipotential surfaces are as plane as possible, and how far this plane lies from the plane containing the wires,

$$z = z_0$$

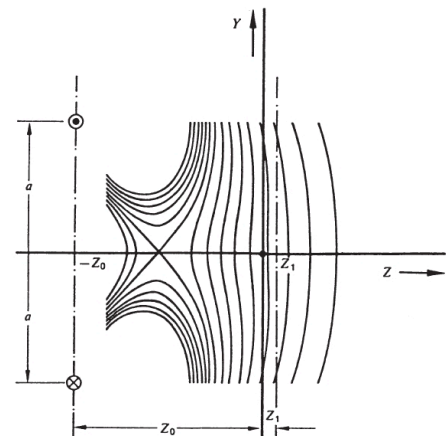


Fig. 3: Lines of constant field inhomogeneity.

Theory (11/31)

To do this, the length of the element of path ($z_0 + z_1$) will be determined, subject to the condition that, in the neighbourhood of $y = 0$, $\partial H / \partial z$ is independent of y .

If one develops $\partial H / \partial z$ in a series of y^2 and breaks this off after the first order, on the assumption that y^2 is small compared with $(z_0 + z_1)^2$ or a^2 , the field gradients are found to be

$$\left| \frac{\partial H}{\partial z} \right|_{z_1} = \frac{2l \cdot a(z_0 + z_1)}{\pi}$$

Dependence on y is to vanish at $z = z_1$. We then get:

$$2a^2 - (z_0 + z_1)^2 = 0$$

Theory (12/31)

from which it follows that

$$z_1 + z_0 = a \cdot \sqrt{2}$$

The field inhomogeneity begins to decrease steeply with increasing y only at greater distances along the z -axis. The present apparatus has a diaphragm system in which the length of the radiation window is about $4/3 a$. As Fig. 4 shows, the value of $\partial H / \partial z$ at $y \approx 2/3 a$ scarcely differs from its value at $y = 0$. The condition for constant inhomogeneity is thus met to a large extent.

Now only H can be measured in the region of the z -axis, and not $\partial H / \partial z$. Hence it is also useful to find that plane for which

$$\left| \frac{\partial H}{\partial z} \right| = \frac{a}{H} = \varepsilon$$

is a value not depending on y in the neighbourhood of $y = 0$.

Theory (13/31)

This plane is to be $z = 0$, i. e., it helps to fix z_0 . Expansion as a series in y^2 gives

$$\varepsilon = \frac{2a(z+z_0)}{a^2+(z+z_0)^2} \left(1 + \frac{y^2}{(a^2+(z+z_0)^2)^2} \cdot (5a^2 - 3(z+z_0)^2) \right)$$

Dependence on y should vanish at $z = 0$. We then get

$$5a^2 - 3z_0^2 = 0$$

from which it follows that

$$z_0 = a\sqrt{\frac{5}{3}} = 1.29a$$

$$\text{Hence } z_1 = \left(\sqrt{2} - \sqrt{\frac{5}{3}} \right) a = 0.12a \ll z_0 \quad (8)$$

Theory (14/31)

The plane $z = z_1$ lies therefore immediately adjacent to the plane $z = 0$. Hence the inhomogeneity at $z = 0$ can be regarded as being constant, to a good approximation.

The Stern-Gerlach apparatus is adjusted, in view of the foregoing relationships, so that the radiation window lies around $1.3a$ from the notional wires of the two-wire system (Figs. 4 and 5).

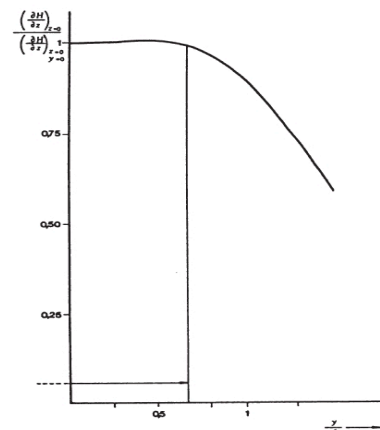


Fig. 4: Behaviour of field inhomogeneity along the radiation window.

Theory (15/31)

PHYWE
excellence in science

The calibration $H(i)$ of the electromagnet (magnetic field H of magnetic induction B against the excitation current i) is likewise assumed for $z \approx 1.3a$ (Fig. 6)

The constant ε can therefore be calculated from

$$\varepsilon(z=0) = \frac{2 \cdot \sqrt{5/3}}{1+5/3} = 0.968$$

Field strengths are therefore converted to field gradients using the equation

$$\left| \frac{\partial H}{\partial z} \right| = 0.968 \frac{H}{a}$$

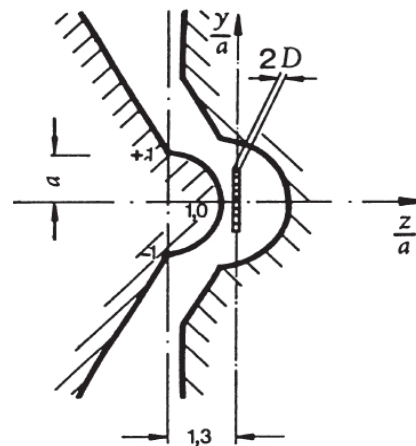


Fig. 5: Position of the atomic beam.

Theory (16/31)

PHYWE
excellence in science

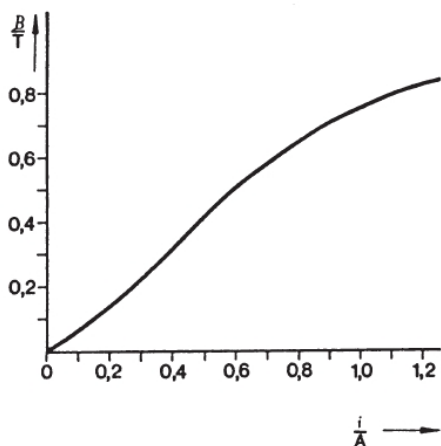


Fig. 6 : Calibration of the electromagnet, according to data sheet.

Particle track

The velocity v of the potassium atoms entering the magnetic field can be considered with sufficient accuracy as being along the same direction (x-direction) before entry into the field. The following transit in the x-direction should be borne in mind (Fig. 7): a time

$$\Delta t = \frac{L}{v}$$

for passing through the magnetic field of length L and a time $t = \frac{l}{v}$

for the distance l from the point of entry into the magnetic field to the point of entry into the plane of the detector.

Theory (17/31)

Because of the effectively constant force in the z-direction, the potassium atoms of mass M acquire, by virtue of the inhomogeneity of the field, a momentum

$$M\dot{z} = F_z \Delta t = \frac{F_2 \cdot L}{v} = \frac{-m\mu_B L}{v} \frac{\partial B}{\partial z}$$

It follows that the point of impact u of a potassium atom of velocity v in the x-direction, at a given field inhomogeneity, is

$$u = \frac{1}{2}\dot{z}\Delta t + \dot{z}(t - \Delta t) = z + \left(1 - \frac{1}{2}\frac{L}{l}\right) \frac{l}{v}\dot{z} \quad (9)$$

where $\frac{1}{2}z\Delta t$

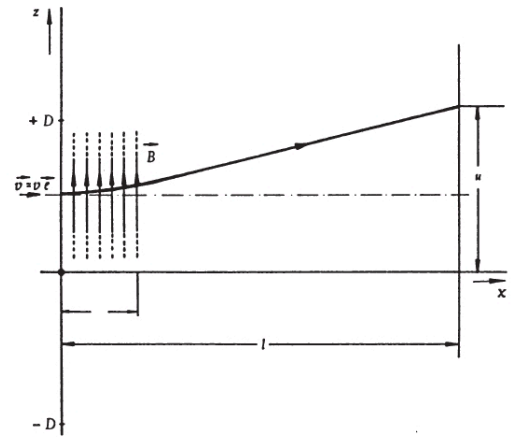


Fig. 7: Particle track between magnetic analyser and detection plane.

Theory (18/31)

is the path element covered by a potassium atom immediately after passing through the magnetic field in the z-direction. Hence, there is the following fundamental relationship between the deflection u , the particle velocity v and the field inhomogeneity $\partial H/\partial z$:

$$u = z - \frac{lL}{Mv^2} \left(1 - \frac{1}{2}\frac{L}{l}\right) m\mu_B \frac{\partial B}{\partial z}$$

where $u - z > 0$ for $m = +\frac{1}{2}$

and $u - z < 0$ for $m = -\frac{1}{2}$

It will be noticed that the faster particles are deflected less from their path than the slower ones.

Theory (19/31)

Velocity distribution

In order to produce a beam of potassium atoms of higher average particle velocity, a furnace heated to a defined temperature T is used. In the furnace, the evaporated potassium atoms are sufficiently numerous to acquire a maxwellian velocity distribution, i.e., the number of atoms with a velocity between v and $v + dv$ in each elementary volume dV of the furnace is proportional to $e^{-\frac{Mv^2}{2kT}} \cdot v^2 dv$

This proportionality applies also when one considers only the velocity directions lying within a solid angle $d\Omega$ which is determined at $x = 0$ by tracks of width dz . The atoms which emerge from the opening in the furnace, and which have entered the magnetic field between z and $z + dz$, with a velocity between v and $v + dv$, obviously satisfy a velocity function involving the third power of v (Fig. 8):

$$d^2n = \frac{\Phi_m(z) e^{-\frac{Mv^2}{2kT}} \cdot v^3 dv dz}{2 \int_0^\infty e^{-\frac{Mv^2}{2kT}} v^3 dv} \quad (10)$$

Theory (20/31)

Thus, only those potassium atoms traverse the strip dz in time dt with velocity v at a later point in time corresponding to the transit time, which come from volume element dV existing in a region at depth vdt behind the opening in the furnace. The volume of this region is proportional to v and contributes likewise to the distribution function. Indexing with m takes account of the two possible magnetic moments of the potassium atom. On symmetry grounds it can be assumed that both directional orientations are equally probable.

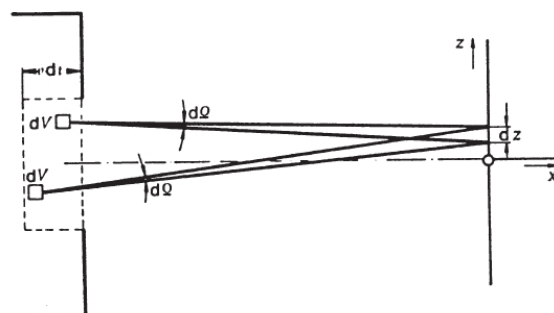


Fig. 8: Geometrical relationships for deriving the distribution function depending on v and z .

Theory (21/31)

The function $\Phi(z)$ represents the spatial profile of the numbers of particles, for particles of orientation m at the position $x = 0$. It arises through limitation of the atomic beam by appropriate systems of diaphragms. The function $\Phi(z)$ differs from zero within a rectangular area of width D (beam enclosure).

Particle current density

The object of the following calculation is to calculate the particle current density I in the measuring plane $x = 0$, as a function of the position u , from the distribution which depends on v and z , since this density is proportional to the signal at the detector. All potassium atoms entering the magnetic field at a height of z are spread by an amount du at position u on account of their differences in velocity dv . For equal values of z , therefore, the following conversion from v to u applies:

$$v^3 dv = \frac{1}{2} \left| \frac{\partial v^4}{\partial u} \right| du$$

Theory (22/31)

From equation (9) for the deflection of the path as a function of v , one obtains by substitution and differentiation:

$$v^2 dv = \frac{1}{2} \left(\frac{IL \left(1 - \frac{1}{2} \frac{L}{l}\right) \mu_B \frac{\partial B}{\partial z}}{2M} \right)^2 \frac{du}{|u-z|^3}$$

In addition, $\frac{Mv^2}{2kT} = \frac{IL \left(1 - \frac{1}{2} \frac{L}{l}\right) \mu_B \frac{\partial B}{\partial z}}{2kT|u-z|}$

If, to abbreviate, we now let

$$q = \frac{IL \left(1 - \frac{1}{2} \frac{L}{l}\right) \mu_B \frac{\partial B}{\partial z}}{2kT} \quad (11)$$

$$\text{and } n_0 = \frac{\left[IL \left(1 - \frac{1}{2} \frac{L}{l}\right) \mu_B \frac{\partial B}{\partial z} \right]^2}{16M^2 \int_0^\infty e^{-\frac{Mv^2}{2kT}} \cdot v^3 dv}$$

we obtain from (10) the distribution

$$d^2n = n_0 \Phi_m(z) \cdot e^{-\frac{q}{|u-z|}} \cdot \frac{du}{|u-z|^3} dz \quad (12)$$

Theory (23/31)

We now integrate with respect to z and sum over the possible orientations m , and so derive the desired particle current density at position u :

$$I = \frac{\sum_m \int_{-D}^{+D} d^2n}{du} = n_0 \int_{-D}^{+D} \Phi_{-1/2}(z) e^{-\frac{q}{|u-z|}} \frac{dz}{|u-z|^3} + n_0 \int_{-D}^{+D} \Phi_{-1/2}(z) e^{-\frac{q}{|u-z|}} \frac{dz}{|u-z|^3}$$

By reason of the equivalence to the particle profile of the orientations $m = -1/2$ and $m = +1/2$,

$$\Phi_{+1/2}(z) \equiv \Phi_{-1/2}(z) I_0(z)$$

$$\text{and hence } I_0 \int_{-D}^{+D} I_0(z) e^{-\frac{q}{|u-z|}} \frac{dz}{|u-z|^3} \quad (13)$$

For a vanishing magnetic field or a vanishing inhomogeneity, $u \equiv z$ and is independent of v . In this case, the particle current density in the measuring plane is defined as $I_0(u)$.

Theory (24/31)

Infinitesimal beam cross-section

The course of the particle current density $I(u)$ depends, among other factors, on how $I_0(u)$ is formed. As the simplest approximation, one can start from a beam enclosure of any desired narrowness:

$$I_0^{(0)}(z) = 2DI_0\delta(z) \quad (14)$$

$$\text{using } \int_{-\infty}^{z_0} \delta(z) dz = \Theta(z_0) = \begin{cases} 0 & \text{for } z_0 < 0 \\ 1 & \text{for } z_0 > 0 \end{cases}$$

as the definition of the Dirac Function δ

Theory (25/31)

We then get

$$I_0^{(0)}(u) = 2Dn_0I_0 \int_{-D}^{+D} \delta(z) e^{-\frac{q}{|u-z|}} \frac{dz}{|u-z|^3}$$

$$\text{and therefore } I_0^{(0)}(u) = 2Dn_0I_0 \frac{e^{-\frac{q}{|u|}}}{|u|^3} \quad (15)$$

The particle current density $I^{(0)}(u)$ for narrow beam profiles is therefore proportional to the width $2D$ determined by the diaphragm system. The position u_e of the intensity maximum is found by differentiating with regard to u :

$$\frac{dI^{(0)}(u)}{du} = 2Du_0I_0 \frac{q-3|u|}{u^5} e^{-\frac{q}{|u|}}$$

Theory (26/31)

From

$$\frac{dI^{(0)}(u)}{du}(u_e^{(0)}) = 0 \quad (16)$$

we obtain the determining equation for $u_e^{(0)}$:

$$u_e^{(0)} = \pm \frac{1}{3}q = \pm \frac{I \cdot L \left(1 - \frac{1}{2} \frac{L}{I} \mu_B \frac{\partial B}{\partial z}\right)}{6kT} \quad (17)$$

The distances of the maxima from the x-axis (beam deflection) therefore increase in proportion to the field inhomogeneity.

Theory (27/31)

A better compatibility of the calculation with the experiment is achieved by regarding the beam enclosure with width $2D$ as being infinitely long, and by describing the beam profile as two steep straight lines with a parabolic apex (Fig. 9).

$$I_0(z) = \delta \begin{cases} D+z & -D \leq z \leq -p \\ D - \frac{1}{2}p - \frac{1}{2}\frac{z^2}{p} & -p \leq z \leq +p \\ D-z & +p \leq z \leq +D \end{cases}$$

$$\frac{dI_0}{dz} = i_0 \begin{cases} 1 & -D \leq z \leq -p \\ -\frac{z}{p} & -p \leq z \leq +p \\ -1 & +p \leq z \leq +D \end{cases} \quad (18)$$

Theory (28/31)

$$\frac{d^2 I_0}{dz^2} = i_0 \begin{cases} 0 & -D \leq z \leq -p \\ -\frac{1}{p} & -p \leq z \leq +p \\ 0 & +p \leq z \leq +D \end{cases}$$

In this model, $I_0(z)$ is regarded as being twice differentiable. The particle current density $I(u)$ based on this supposition has values, dependent on the inhomogeneity of the magnetic field and hence on q , which have maxima at positions $u_e(q)$, which differ to a greater or lesser extent from the positions $u_e^{(0)} = \pm q/3$ resulting from the approximation assuming an infinitesimally narrow beam enclosure.

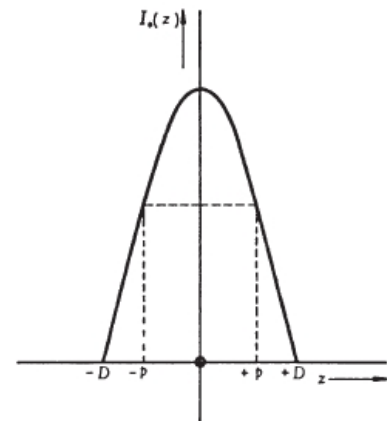


Fig. 9: Mathematical assumption of particle current density with a vanishingly-small magnetic field.

Theory (29/31)

To determine the function $u_e(q)$ we start from the condition

$$\frac{dI}{du}(u_e) = 0 \quad (19)$$

In calculating dI/du , the differentiation after u can be incorporated within the integral, as can be readily seen in the behaviour of the integrand for $z \rightarrow u$:

$$\frac{dI}{du} = \frac{d}{du} n_{0m} \int_{-D}^{+D} dz I_0(z) \frac{e^{-\frac{q}{|u-z|}}}{|u-z|^3} = n_0 \int_{-D}^{+D} dz I_0(z) \frac{\partial}{\partial u} \frac{e^{-\frac{q}{|u-z|}}}{|u-z|^3}$$

The integrand is not changed if $\frac{\partial}{\partial u}$ is replaced by $-\frac{\partial}{\partial z}$.

Theory (30/31)

The differentiation with regard to I_0 can now be shifted by partial integration:

$$\frac{dI}{du} = n_0 \int_{-D}^{+D} dz \frac{dI_0}{(dz)} \cdot \frac{e^{-\frac{q}{|u-z|}}}{|u-z|^3} = n_0 i_0 \int_{-D}^{+P} dz - \frac{u}{p} \int_{-P}^{+P} dz - \int_{+P}^{+D} dz \cdot \frac{e^{-\frac{q}{|u-z|}}}{|u-z|^3}$$

$$n_0 i_0 = \frac{1}{P} \int_{-P}^{+P} dz \frac{u-z}{|u-z|^3} \cdot e^{-\frac{q}{|u-z|}}$$

The integrals occurring here can be solved in stages. We get $\frac{dI}{du} = \frac{n_0 i_0}{pq^2} \cdot F(u)$ (20)

with the solution function

$$F(u) = -|u+p| \cdot e^{-\frac{q}{|u-p|}} + |u-p| \cdot e^{-\frac{q}{|u-p|}} + p \frac{q+|u+D|}{u+D} \cdot e^{-\frac{q}{|u-p|}} + p \frac{q+|u-D|}{u-D} \cdot e^{-\frac{q}{|u-D|}} \quad (21)$$

Theory (31/31)

From this, there follows immediately the determining function sought, for the position of the particle current maximum:

$$F(u_e) = 0 \quad (22)$$

From the central symmetry for $f(u_e)$ there results the mirror symmetry of the solution curve $u_e(q)$. It is therefore sufficient to restrict the evaluation to positive u_e .

Equipment

Position	Material	Item No.	Quantity
1	Stern-Gerlach apparatus	09054-88	1
2	Matching transformer	09054-04	1
3	Electromagnet w/o pole shoes	06480-01	1
4	Pole piece, plane	06480-02	2
5	High vacuum pump assembly, compact	09059-99	1
6	Ultra-Low-Noise Current Amplifier	13627-99	1
7	PHYWE power supply, variable DC: 12 V, 5 A / AC: 15 V, 5 A	13540-93	1
8	PHYWE Power supply, 230 V, DC: 0...12 V, 2 A / AC: 6 V, 12 V, 5 A	13506-93	2
9	Digital thermometer, -50...+1300°C, for type K and J sensor	07022-00	1
10	Commutator switch	06006-00	1
11	Adapter, BNC male/4 mm female pair	07542-26	1
12	Potassium ampoules, set of 6	09054-05	1
13	Isopropyl alcohol, extra pure, 1000 ml	30092-70	1
14	Steel cylinder, nitrogen, 10l, full	41763-00	1
15	Reducing valve f. nitrogen	33483-00	1
16	Rubber tubing, vacuum, i.d. 6mm	39286-00	3
17	Gas-cylinder Trolley for 10 L.	41790-10	1
18	Two-tier platform support	02076-03	1
19	Storage tray, 413 x 240 x 100 mm	47325-02	1
20	Cristallizing dish, boro3.3, d = 200 mm	46246-00	1
21	Connecting cord, 32 A, 250 mm, blue	07360-04	2
22	Connecting cord, 32 A, 250 mm, yellow	07360-02	2
23	Connecting cord, 32 A, 500 mm, red	07361-01	3
24	Connecting cord, 32 A, 500 mm, blue	07361-04	2
25	Connecting cord, 32 A, 500 mm, green-yellow	07361-15	1
26	Connecting cord, 32 A, 750 mm, red	07362-01	1
27	Connecting cord, 32 A, 750 mm, yellow	07362-02	3
28	PHYWE Demo Multimeter ADM 3: current, voltage, resistance, temperature	13840-00	4
29	Frame for complete experiments	45500-00	2
30	Shelf with hanging device	45505-00	2
31	Stange, genutet, L=285 mm	315843	2



Setup and Procedure

Setup and Procedure (1/7)

1. Preparation of vacuum system: evacuation

Connection of the two-stage rotary pump (backing pump) to the vacuum valve, using metallic hose. Connection of the prevacuum pressure gauge to the pre-vacuum measuring point (Fig. 10).

Before starting up the Stern-Gerlach apparatus for the first time, or after a long period out of action, the pump stand should first be evacuated (switch on vacuum pump, open prevacuum and mainvacuum valves). When the pressure has fallen to 100 mPa, close the valves (backing pump can be switched off) and start using the iongetter-pump.

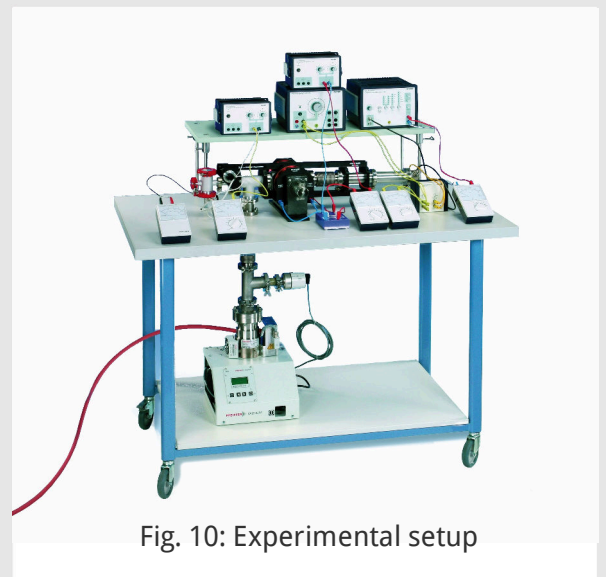


Fig. 10: Experimental setup

Setup and Procedure (2/7)

Proceed in the following steps: start with an ion current range multiplier up to 200 mA, set the commutator switch to "Start", and operate the mains switch. When the ion current has fallen to below 10 mA, set the commutator switch to "Protect". A safety system is thereby connected, which will switch off the pump if gas leaks in. When the ion current has fallen to less than 1.5 mA, switch off the pump (set the commutator switch to "Start", and disconnect from the mains).

2. Preparation of the vacuum installation: filling

Disconnect current supply to detector. Set the pressure-regulating valve of the nitrogen cylinder to as near below 500 hPa as possible. Open the gas cylinder and fitting and then connect to the filling valve of the pump stand. Open the main valve. Nitrogen flows in.

Setup and Procedure (3/7)

3. Assembly of the Stern-Gerlach apparatus

Uncover the blank flange on the connecting piece to the Stern-Gerlach apparatus while the nitrogen is flowing (only remove the clamping ring, do not lift the flange out). Allow the nitrogen to continue to flow in: the blank flange will be easily lifted after a short time by the pressure of the nitrogen and nitrogen will leak out by intermittent to-and-fro movements. Uncover the blank flange of the potassium furnace by removing the red locking ring, but do not remove the flange. Remove the blank flange of the connecting piece from the vacuum installation, but take care that the blank flange does not fall off/in to the furnace. Remove the uncovering blank flange of the pump stand and immediately attach the Stern-Gerlach apparatus and secure it by the locking ring.

Now evacuate the apparatus. To do this, connect up the vacuum pump and then, after a short interval, shut off the flow valve and open the pre-vacuum valve. Close the valves when the pressure has fallen to 100 mPa (the backing pump can be disconnected). Restart the ion getter pump (the range multiplier for the ion current first being 200 mA, the commutator switch set at "Start", and the mains connected up). When the ion current falls to 10 mA, set commutator switch to "Protect".

Setup and Procedure (4/7)

PHYWE
excellence in science

4. Charging the atomic beam furnace

Uncover the blank flange of the furnace after removing in the red locking ring, but do not remove this flange. Flush the apparatus with nitrogen as already described (see 2).

When the blank flange of the atomic beam furnace starts moving to-and-fro, the flange can be removed. Insert the key for releasing the furnace-opening locking screw and turn the screw to remove it. Then replace the blank flange.

Place a potassium ampoule with its tip upwards into the steel cylinder of the ampoule opener and cover it with its associated steel disc. Strike the steel disc with a hammer, thus cutting off the top of the ampoule. Caution when handling potassium! Contact with the skin causes burns. Wear protective goggles! After their use, throw any parts with have been wetted by potassium into a vessel containing propanol-2.

Setup and Procedure (5/7)

PHYWE
excellence in science

While all protective measures are taken, the potassium injector must be turned as quickly as possible in the opened ampoule as far as it will go in order to remove the potassium.

Withdraw the injector, strip off glass splinters with a spatula, remove the blank flange of the atomic beam furnace, hold the injector inside the furnace, shake out the potassium, and ram the injector securely into the bottom of the furnace. Re-insert the furnace locking screw and place the blank flange over it.

Caution! All parts wetted with potassium must be thrown into the vessel containing propanol-2. Do not take them out again until the reaction is complete.

Setup and Procedure (6/7)


 PHYWE
 excellence in science

5. Evacuation on the Stern-Gerlach apparatus

After pumping out the equipment with the backing pump, with the atomic beam furnace heater switched on (supply voltage 4 to 5 V AC in accordance with the data sheet in the operating instructions), evacuate the furnace until the ion current falls to below 0.5 mA. This operation may possibly take several hours! It is advisable to connect up the detector current supply at this point (supply voltage as in data sheet).

If need be, after the charging is complete, re-tighten the red locking ring of the blank flange of the atomic beam furnace.

6. Preparation of the magnet electric circuit

Pull apart the pole pieces of the magnet with tightening screws, position the magnet on its associated base support so that the gap between the pole pieces faces the detector, and push it towards the magnetic analyser. Adjust the magnet so that the front of the pole pieces lies parallel to the outer face of the Stern-Gerlach pole pieces. Secure the pole pieces against these faces.

Setup and Procedure (7/7)


 PHYWE
 excellence in science

The electrical circuit is shown in Fig.11. To carry out a measurement demagnetize the electromagnet. This is done by reducing the excitation current in steps by small amounts, reversing the polarity at each step using the commutating switch.

7. Carrying out the experiment

When carrying out an experiment, make sure that the voltages applied to the atomic beam furnace and the matching transformer correspond to those given in the data sheet. Check the heating voltage. When making a series of measurements by changing the position of the detector always turn the micrometer screw in one direction only. The geometrical data of the apparatus required for evaluation are likewise specified in the data sheet.

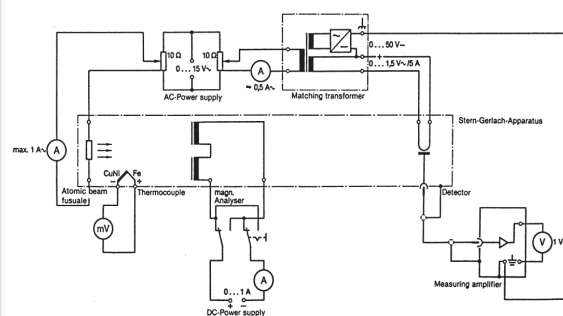
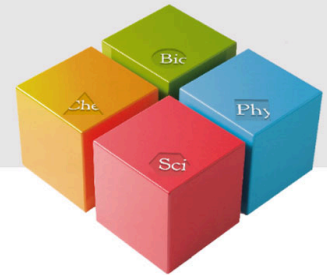


Fig. 11: Electrical circuit.



Evaluation

Results (1/13)

Measurement of particle current density with vanishing small magnetic field

Fig. 12 shows the particle current density taken up by the detector (ionization current I_i in pA) as a function of the point of measurement u , in the absence of a magnetic field. It is not necessary in this case to determine the zero for u . When the course of the curve is fitted by the straight lines and the parabolic segment, one obtains the following characteristic values:

$p = 0.20$ scale div. = 0.36 mm, $D = 0.48$ scale div. = 0.86 mm.

The value for $2D$ corresponds to the width of the beam enclosure to be set under the condition of a parallel atomic beam.

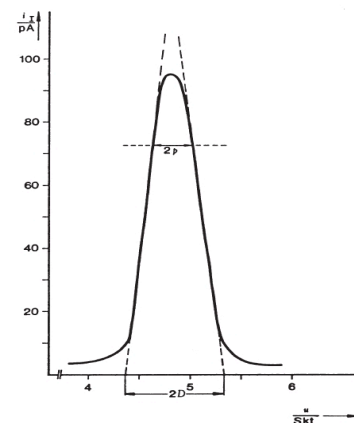


Fig. 12: Ionisation current as a function of the point of measurement u with a vanishingly-small magnetic field.

Results (2/13)

Calculation of the position of the intensity maximum

When these dimensions are used, the function $F(u)$ in equation (21) gives a curve strongly influenced by q (Fig. 13):

The points of intersection u_e with the u -axis give the relation between u_e and q to be expected from the calculation (Fig. 14).

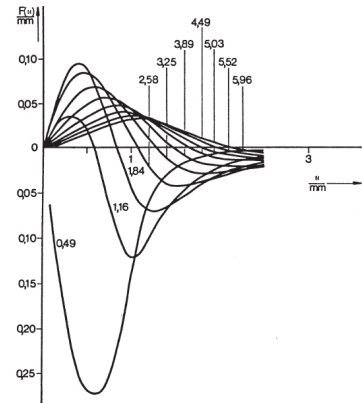


Fig. 13: Solution function $F(u)$ for various parameters q . The numbers 0.49 to 5.96 correspond to q in mm.

Results (3/13)

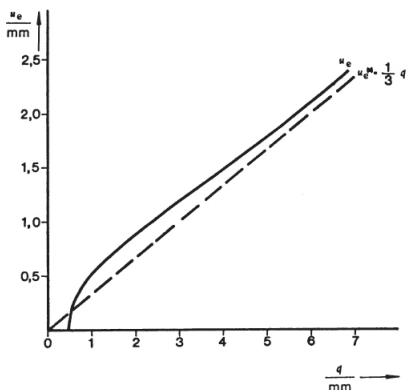


Fig. 14: Position u_e of the zero point of the solution function $F(u)$ as a function of the parameter q .

Calculation of the asymptotic behaviour with large fields

For a sufficiently large field inhomogeneity, u_e approaches the solution given by a progressively smaller (infinitesimal) beam enclosure. The following calculation provides the more accurate course of the function $u_e(q)$ for larger fields. Since it is assumed here that

$$\frac{u_e}{p}, \frac{u_e}{D}, \frac{q}{p}, \frac{q}{D} \ll 1 \quad (23)$$

a Taylor series for $F(u)$ can be developed. To do this, we require the function

$$f(u) = u \cdot e^{-\frac{q}{u}}$$

Results (4/13)

and its derivatives as follows:

$$f^{(3)}(u) = \frac{q^2}{u^4} \left(\frac{q}{u} - 3 \right) e^{-\frac{q}{u}}$$

$$f^{(5)}(u) = 12 \frac{q^2}{u^6} \left(5 \left(\frac{q}{u} - 1 \right) + \frac{1}{12} \frac{q^2}{u^2} \left(\frac{q}{u} - 15 \right) \right) e^{-\frac{q}{u}}$$

Up to the sixth derivative of $f(u)$ only the coefficients of the third and fifth derivatives do not cancel each other out in $F(u)$.

The Taylor series is broken off above the sixth derivative.

$$F(u) = p \left(D^2 - \frac{1}{3} p^2 \right) \cdot f^{(3)}(u) + \frac{p}{12} \left(D^4 - \frac{1}{5} p^4 \right) \cdot f^{(5)}(u) + \dots \quad (24)$$

Results (5/13)

The determining equation for u_e

$$0 = \left(D^2 - \frac{1}{3} p^2 \right) \left(\frac{q}{u_e} - 3 \right) + \frac{D^4 - \frac{1}{5} p^4}{u_e^2} \left(5 \left(\frac{q}{u_e} - 1 \right) + \frac{1}{12} \frac{q}{u_e^2} \left(\frac{q^2}{u_e} - 15 \right) \right)$$

is thus obtained.

The summand on the left gives the known solution $u_e^{(0)} = \pm q/3$ if the summand on the right is disregarded. When this is not done, it is permissible to replace u_e by $u_e^{(0)}$ in the summand on the right, because the associated difference is of a still higher order.

Results (6/13)

The quantity in parentheses on the right becomes unity:

$$0 = \left(D^2 - \frac{1}{3}p^2\right) \left(\frac{q}{u_e} - 3\right) + \frac{D^4 - \frac{1}{5}p^4}{u_e^2}$$

This equation leads to

$$q = 3u_e + \frac{D^4 - \frac{1}{5}p^4}{D^2 - \frac{1}{3}p^2} \cdot \frac{1}{u_e} \quad (25)$$

$$\text{or } u_e = \frac{q}{3} + \frac{D^4 - \frac{1}{5}p^4}{D^2 - \frac{1}{3}p^2} \cdot \frac{1}{q} \quad (26)$$

as an approximation for sufficiently larger inhomogeneous fields.

Results (7/13)

I	$\partial B/\partial z$
0	0
0.095	25.6
0.200	58.4
0.302	92.9
0.405	132.2
0.498	164.2
0.600	196.3
0.700	226.0
0.800	253.7
0.902	277.2
1.010	298.6

Table

Measurements of particle current density

The graphs in Figs. 15 and 16 show the particle current densities (measured as ionization currents I_i) in a series of measurements of different excitation currents i of the field magnet.

The asymmetry in height of the intensity maxima is connected with the fact that the inhomogeneity of the magnetic field is slightly different to the left and the right of the beam enclosure.

The field inhomogeneities at the different excitation currents, according to the calibration curves of the magnet, are given in the following Table: (current i in A; $-\partial B/\partial z$ in T/m):

Results (8/13)

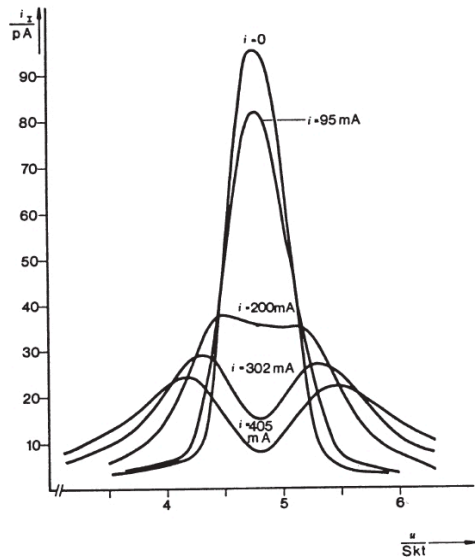


Fig. 15: Ionisation current as a function of position (u) of detector with small excitation currents in the magnetic analyser.

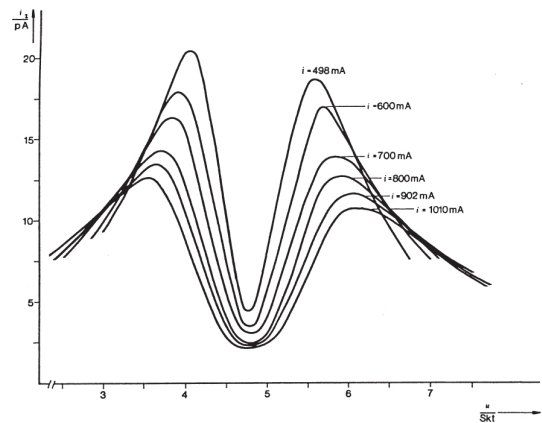


Fig. 16: Ionisation current as a function of position (u) of detector with large excitation currents in the magnetic analyser.

Results (9/13)

The positions of the intensity maxima shown in Figs. 15 and 16 are shown in Fig. 17 as a function of the inhomogeneity $\partial B/\partial z$

Evaluation in the asymptotic limiting case

The graph in Fig. 18 shows $\partial B/\partial z$ as a function of the expression

$$q = 3u_e - \frac{c}{u_e}$$

$$\text{where } c = \frac{D^4 - \frac{1}{5}p^4}{D^2 - \frac{1}{3}p^2} = 0.781 \text{ mm} \quad (27)$$

(cf. Equation 25).

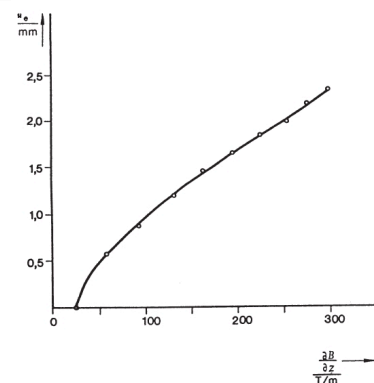


Fig. 17: Experimentally determined relationship between the position u_e of the particle current density maximum and the magnetic field inhomogeneity.

Results (10/13)

PHYWE
excellence in science

From the regression line through the measured values shown in Fig. 18 above the horizontal broken line (within the framework of the permitted approximation in the asymptotic limiting case), together with the exponential equation

$$\frac{\partial B}{\partial z} = A \left(3u_e - \frac{C}{u_e} \right)^B$$

we derive the exponent $B = 1.00$

with the standard error $S.D.(B) = 0.01$.

The slope of the straight line in Fig. 18 is $A = 44.8 \frac{T/m}{mm}$

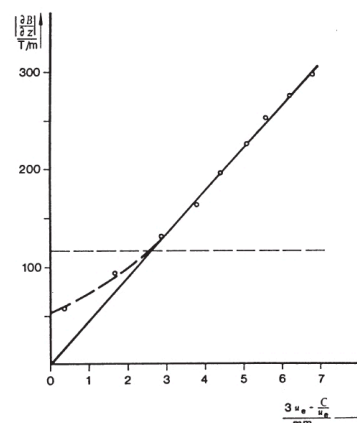


Fig. 18: Field inhomogeneity as a function of u_e . Determination of slope from asymptotic behaviour.

Results (11/13)

PHYWE
excellence in science

Determination of the Bohr magneton

Using the values $l = 0.455$ m, $L = 7$ cm, $a = 2.5$ mm,

The measured value $T = 453$ K,

and the slope of the straight line in Fig. 18, we calculate for the Bohr magneton, in accordance with equations (11), (25) and (27), the value

$$\mu_B = \frac{2kT}{lL \left(1 - \frac{1}{2} \frac{L}{l} \right)} \cdot \frac{3u_e - \frac{C}{u_e}}{\frac{\partial B}{\partial z}} = \frac{2kT}{lL \left(1 - \frac{1}{2} \frac{L}{l} \right) \cdot A} = 9.51 \cdot 10^{-24} \text{ Am}$$

The departure of about 2.5% from the value in the literature is mainly attributable to the inaccuracy of calibration of the magnetic field.

Results (12/13)

PHYWE
excellence in science

Position of intensity maxima as a function of field inhomogeneity

From the asymptotic behaviour of u_e at large values of field inhomogeneity $\partial B/\partial z$ the experiment gives, for the variable q :

$$\frac{q}{-\partial B/\partial z} = \frac{1}{A} = 0.0223 \cdot 10^{-3} m^2 T^{-1}$$

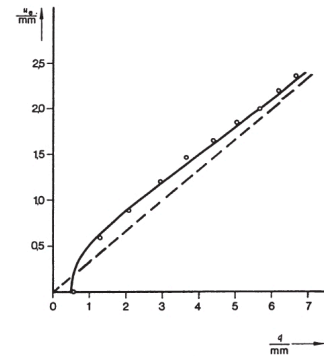


Fig. 19: Measured values for the position u_e of the particle beam current maxima as a function of the variable q , in comparison with theory, represented by the continuous curve.

Results (13/13)

PHYWE
excellence in science

If the positions u_e of the intensity maxima as a function of q are shown complete in accordance with Figs. 15 and 16, the measured points result as in Fig. 19. The theoretically determined relationship is indicated by a continuous line. It is to be noticed that the course of particle current density at low fields, for both spin directions, is only so little deformed relative to the central axis that on superposition the maximum remains on the central axis.

As the inhomogeneities become greater the two maxima appear (suddenly) to the right and left of the central axis. If the inhomogeneities become even greater, the splitting changes in proportion to the inhomogeneity.